Supporting Information

Smith et al. 10.1073/pnas.1214062110

SI Materials and Methods

Electrophysiology Experiments with Exogenously Expressed Receptors in *Xenopus* Oocytes. ***Expression of voltage-gated ion channels in*** **Xenopus laevis** ***oocytes.*** For the expression of the voltage-gated potassium channels [rK_V1.1, rK_V1.2, hK_V1.3, rK_V1.4, rK_V1.5, rK_V1.6, *Shaker* IR, rK_V2.1, hK_V3.1, rK_V4.2, rK_V4.3, human Ether-à-go-go-Related Gene (hERG)], the voltage-gated sodium channels (rNa_V1.2, rNa_V1.3, rNa_V1.4, hNa_V1.5, rNa_V1.7, rNa_V1.8, rβ1, hβ1, and the insect channel DmNa_V1), and the voltage-gated calcium channels (rCa_V3.3) in *Xenopus* oocytes, the linearized plasmids were transcribed using the T7 or SP6 mMESSAGE-mMACHINE transcription kit (Ambion). The harvesting of stage V–VI oocytes from anesthetized female *Xenopus laevis* frog was previously described (1). Oocytes were injected with 50 nL of cRNA at a concentration of 1 ng/nL using a microinjector (Drummond Scientific). The oocytes were incubated in a solution containing (in mM): NaCl, 96; KCl, 2; $CaCl_2$, 1.8; $MgCl_2$, 2 and Hepes, 5 (pH 7.4), supplemented with 50 mg/L gentamycin sulfate.

Electrophysiological recordings. Two-electrode voltage-clamp recordings were performed at room temperature (18–22 °C) using a Geneclamp 500 amplifier (Molecular Devices) controlled by a pClamp data acquisition system (Axon Instruments). Whole-cell currents from oocytes were recorded 1–4 d after injection. Bath solution composition was ND96 (in mM): NaCl, 96; KCl, 2; $CaCl_2$, 1.8; $MgCl_2$, 2 and Hepes, 5 (pH 7.4) or for measuring calcium channels: $BaCl_2$, 10; NaOH, 90; KOH, 1; EDTA, 0.1; and Hepes 5 (pH 7.4). Voltage and current electrodes were filled with 3M KCl. Resistances of both electrodes were kept between 0.5 and 1.5 MΩ. The elicited currents were filtered at 1 kHz and sampled at 0.5 kHz (for potassium currents), 2 kHz (for sodium currents), or at 2.5 kHz (for calcium currents) using a four-pole low-pass Bessel filter. Leak subtraction was performed using a -P/4 protocol. K_V1.1-K_V1.6 and *Shaker* IR currents were evoked by 500-ms depolarizations to 0 mV followed by a 500-ms pulse to −50 mV, from a holding potential of −90 mV. Current traces of hERG channels were elicited by applying a +40 mV prepulse for 2 s followed by a step to −120 mV for 2 s. K_V2.1, K_V3.1, and K_V4.2, K_V4.3 currents were elicited by 500-ms pulses to +20 mV from a holding potential of −90 mV. Sodium current traces were, from a holding potential of −90 mV, evoked by 100-ms depolariarions to V_{max} (the voltage corresponding to maximal sodium current in control conditions). From a holding potential of −90 mV, Ca_V3.3 channel currents, carried by 10 mM $Ba2^+$, were elicited by 100-ms-long test depolarizations applied from 60 to +10 mV or +30 mV. To investigate the current–voltage relationship, current traces were evoked by 5 mV depolarization steps from a holding potential of −90 mV.

High Content Imaging of Cultured Rat Dorsal Root Ganglia Neurons. Dissociated dorsal root ganglia (DRG) neurons were loaded with 5 μM Fura-2-AM (Invitrogen) in physiological salt solution (PSS; composition: NaCl 140 mM, glucose 11.5 mM, KCl 5.9 mM, $MgCl_2$ 1.4 mM, NaH_2PO_4 1.2 mM, $NaHCO_3$ 5 mM, $CaCl_2$ 1.8 mM, Hepes 10 mM) containing 0.3% BSA for 30 min at 37 °C. To remove extracellular dye and facilitate deesterification, cells were washed twice for 5 min with PSS before addition of 90 μL PSS per well and transfer to the recording chamber of the high content imaging platform BD Pathway 855 (BD Biosciences). Wild-type φ-liotoxin-Lw1a (φ-LITX-Lw1a) toxin was added as 10× concentrated stock solutions (210 μM) in a volume of 10 μL, and fluorescence responses (excitation 340 and 380 nm, dichroic filter 400DCLP, emission filter 435LP) were monitored for 120 s with a Hamamatsu Orca ER cooled CCD camera and 10× objective at 22 °C. Addition of ionomycin (100 μM) was used as a positive control to confirm cell viability.

Regions of interest (ROIs) were digitally defined using BD AttoVision Software. Only clearly defined ROIs corresponding to single cells were used for analysis. Ca^{2+} responses to addition of wild-type φ-LITX-Lw1a, expressed as R340/380, were plotted using GraphPad Prism 4. n = 3 wells, with 50, 61, and 26 ROIs.

Electrophysiological Recordings. All data represent at least three independent experiments ($n \geq 3$) and are presented as mean ± SE.

1. Liman ER, Tytgat J, Hess P (1992) Subunit stoichiometry of a mammalian K+ channel determined by construction of multimeric cDNAs. *Neuron* 9(5):861–871.

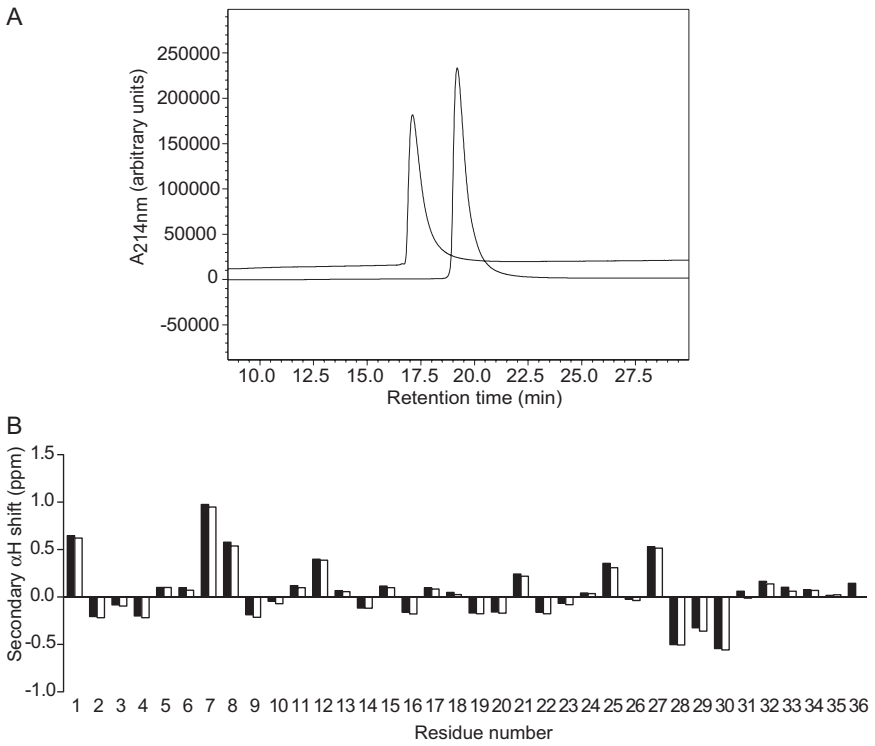

Fig. S1. Synthesis and secondary Hα shift plot of φ-LITX-Lw1a W36A mutant peptide. (*A*) Analytical rpHPLC chromatograms of synthetic reduced (right peak, eluting at ~26% solvent B) and oxidized (left peak, eluting at ~24% solvent B). (*B*) Wild-type φ-LITX-Lw1a analysis in black bars, φ-LITX-Lw1a W36A mutant analysis in white bars.

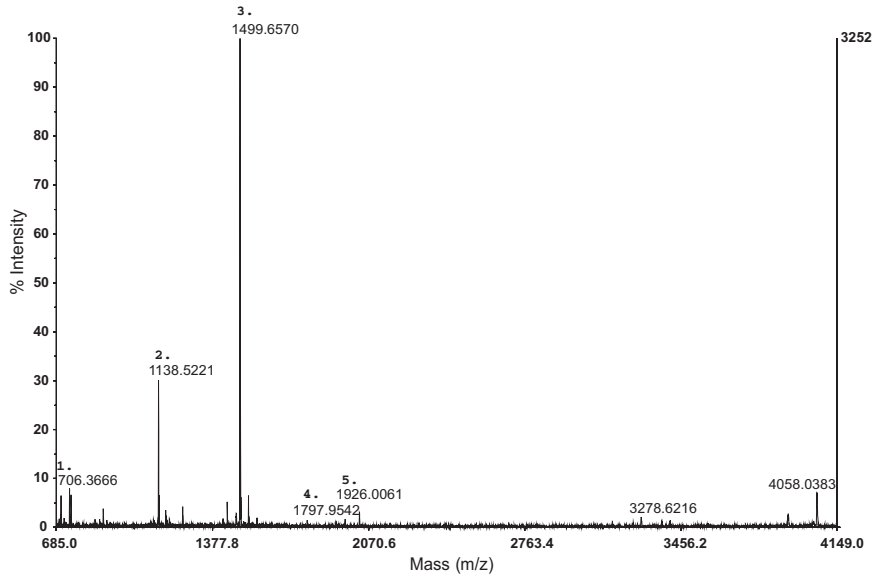

DFPLSKEYESCVRPRKCKPPLKCNKAQICVDPNKGA

Fragment #			Mass [M+H]+(Da) calculated	observed
	1	DFPLSK	706.37	706.37
	2	EYESCVRPR	1138.52	1138.52
	3	EYESCVRPR CNK	1499.65	1499.66
	4	KCKPPLK AQICVDPNK	1797.95	1797.95
	5	KCKPPLK AQICVDPNKGA	1926.01	1926.01

Fig. S2. Disulfide bond determination of φ-LITX-Lw1a W36A mutant. Matrix assisted laser desorption ionization–time of flight spectra of peptide fragments resulting from a tryptic digest of the peptide with intact disulfide bonds. Numbers above the masses in the mass spectrum correspond to the peptide digestion fragment numbers in the table below. The amino acid sequence corresponding to each mass is written next to each fragment number, with the observed and calculated masses listed in the table. The masses three to five are consistent with two peptide fragments joined by a single disulfide bond, hence the disulfide bond connectivity of the full peptide can be ascertained as 1–3, 2–4.

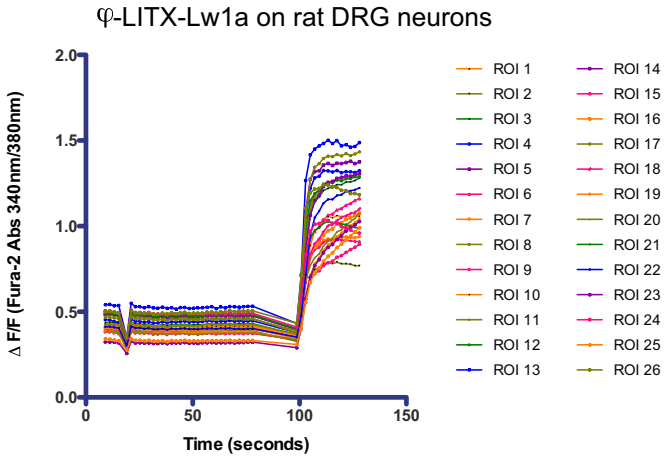

Fig. S3. Rat DRG neuronal assay. Experiment performed in triplicate; however, data from only one replicate shown above because results were equivalent to the other two replicates. Each line represents one cell per ROI. φ-LITX-Lw1a (21 μM) was added at 15 s; ionomycin added as a positive control at 100 s. No response observed in any ROI until the addition of the positive control.

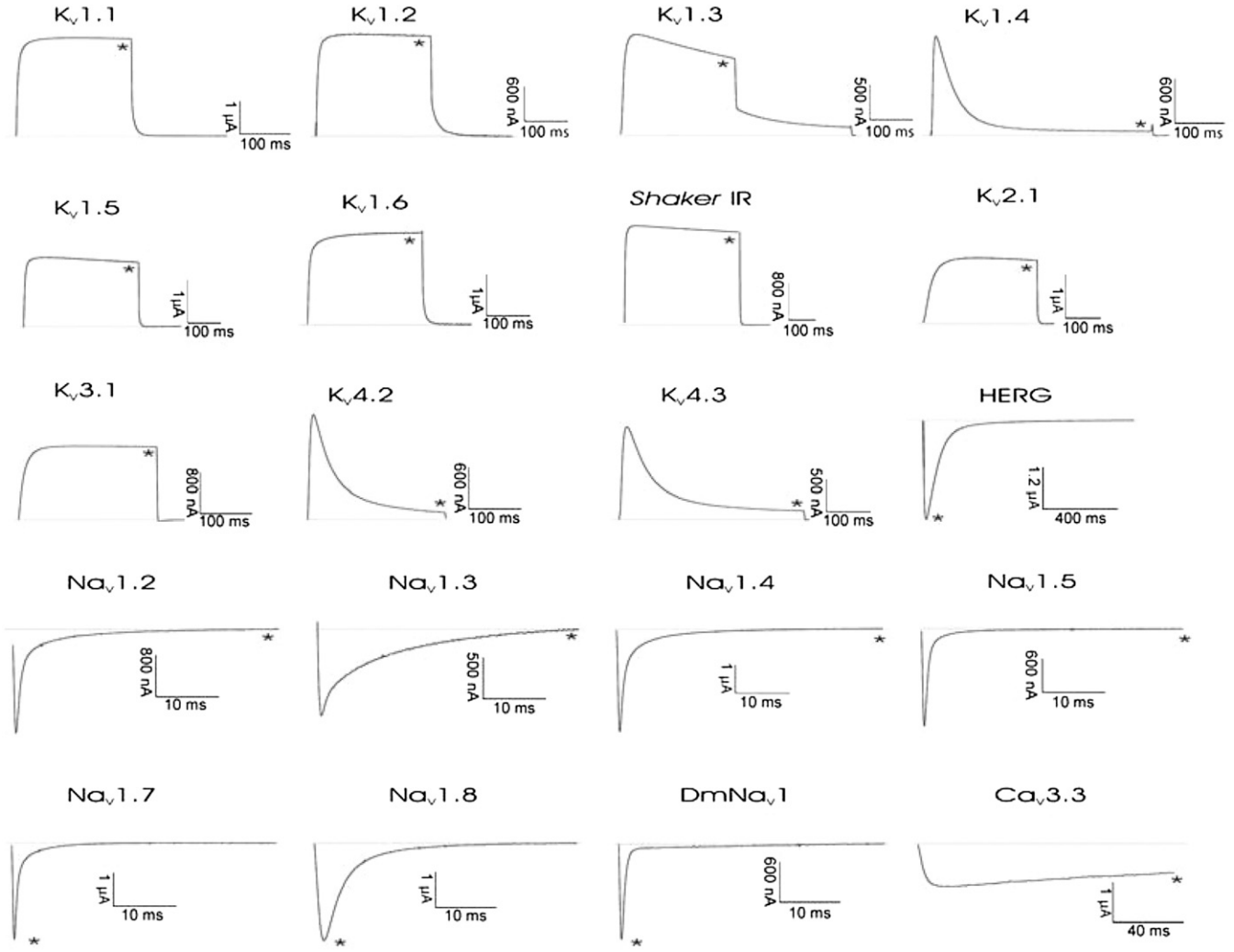

Fig. S4. Electrophysiology experiments with exogenously expressed ion channels in *Xenopus* oocytes. Activity profile of φ-LITX-Lw1a on several K_V, Na_V, and Ca_V channel isoforms. Representative whole-cell current traces in control and toxin conditions are shown. The dotted line indicates the zero-current level. *Steady-state current traces after application of 20 μM toxin. Traces shown are representative traces of at least three independent experiments ($n \geq 3$). $rK_V1.1$, $rK_V1.2$, $hK_V1.3$, $rK_V1.4$, $rK_V1.5$, $rK_V1.6$, and *Shaker* IR currents were evoked by 500-ms depolarizations to 0 mV followed by a 500-ms pulse to −50 mV, from a holding potential of −90 mV. Current traces of hERG channels were elicited by applying a +40 mV prepulse for 2 s followed by a step to −120 mV for 2 s. $rK_V2.1$, $hK_V3.1$ and $rK_V4.2$, $rK_V4.3$ currents were elicited by 500-ms pulses to +20 mV from a holding potential of −90 mV. $rNa_V1.2$-$rNa_V1.4$, $hNa_V1.5$, $rNa_V1.7$, $hNa_V1.8$, and $DmNa_V1$ current traces were, from a holding potential of −90 mV, evoked by 100-ms depolariarions to V_{max} (the voltage corresponding to maximal sodium current in control conditions). All sodium channels α subunits were coexpressed with their appropriate auxiliary subunit (hβ1, rβ1, or TipE). From a holding potential of −90 mV, $rCa_V3.3$ channel currents, carried by 10 mM $Ba2^+$, were elicited by 100-ms-long test depolarizations applied from −60 to +10 mV.

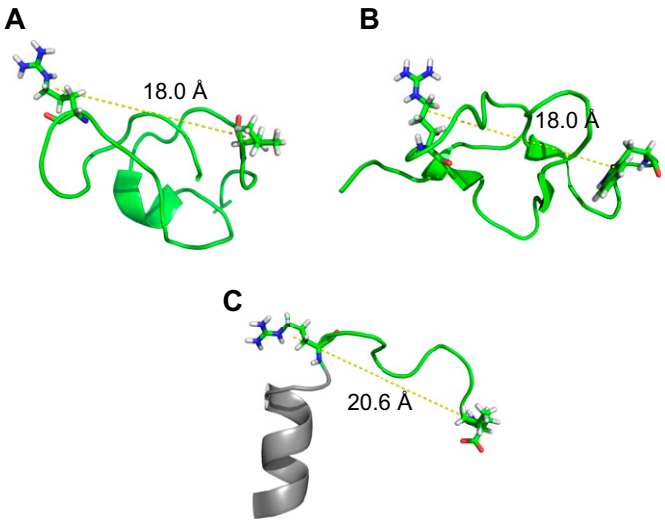

Fig. S5. Structural representations of (*A*) imperatoxin A [Protein Data Bank (PDB) ID 1IE6], (*B*) wild-type φLITX (PDB ID 2KYJ), and (*C*) peptide fragment Thr671-Leu690 of the rabbit skeletal dihydropyridine receptor (DHPR) (PDB ID 1DU1). The peptide backbones are shown as cartoon representations in green. Side chains of Arg24 and Leu7 of imperatoxin A, Arg15, and Trp36 of wild-type φLITX and Arg681 and Leu690 of DHPR segment represented as sticks. The dotted yellow line shows the distance between the centers of geometry of the two residues in each structure. The gray region of the DHPR segment represents the backbone of the nonessential region. Structural representations were prepared using Pymol.

Table S1. Actions of LITX on the overall gating properties of RyR2 and RyR1 channels

Variable	P_o/rel P_o	T_o (ms)/rel T_o	T_c (ms)/rel T_c
Cardiac RyR2			
Control (28)	0.087 ± 0.029	4.0 ± 0.6	179 ± 58
[LITX]			
1 fM (8)	1.4 ± 0.6*	1.9 ± 0.6*	1.9 ± 1.1*
10 fM (10)	1.7 ± 0.7*	2.3 ± 0.6*	0.7 ± 0.3*
100 fM (12)	4.5 ± 1.9*	5.1 ± 1.8*	0.8 ± 0.3*
1 pM (16)	3.3 ± 1.1*	3.5 ± 1.0*	0.9 ± 0.3*
10 pM (18)	5.4 ± 1.4*	2.6 ± 0.3*	0.8 ± 0.4*
100 pM (16)	7.3 ± 2.1*	5.2 ± 2.0*	0.9 ± 0.4*
1 nM (14)	7.9 ± 1.7*	6.6 ± 2.4*	0.7 ± 0.5*
10 nM (4)	8.2 ± 1.9*	2.9 ± 0.6*	0.2 ± 0.1
Skeletal RyR1			
Control (30)	0.046 ± 0.015	2.8 ± 0.4	505 ± 137
[LITX]			
1 fM (10)	2.1 ± 0.3*	1.4 ± 0.2*	0.7 ± 0.1*
10 fM (13)	7.9 ± 3.5*	1.6 ± 0.3*	0.7 ± 0.2*
100 fM (12)	7.6 ± 2.9*	1.6 ± 0.4	0.6 ± 0.1*
1 pM (9)	5.0 ± 3.3*	1.5 ± 0.3*	0.7 ± 0.2*
10 pM (8)	3.7 ± 1.3*	1.7 ± 0.3*	0.5 ± 0.1*
100 pM (8)	4.6 ± 1.2*	1.9 ± 0.3*	0.4 ± 0.1*
1 nM (5)	6.6 ± 1.7*	1.8 ± 0.4*	0.3 ± 0.1*
10 nM (3)	6.6 ± 3.1*	1.6 ± 0.7	0.8 ± 0.5*

The average absolute values for open probability (P_o), mean open time (T_o), and mean closed time (T_c), before toxin addition (control), are given in the first row. The effect of LITX was assessed as the parameter value (e.g., P_oT) in the presence of indicated concentrations of toxin, divided by the control value (P_oC), to give the relative value (e.g., rel P_o). The relative changes in each parameter were determined for each individual channel and then average relative values calculated. Data obtained at +40 mV and −40 mV were combined because the graphs in Fig. 3 indicate similar effects of the toxin at each potential.

*Significant change from the control parameter value in the presence of the toxin.

Table S2. Effect of LITX on the frequency of submaximal conductance openings calculated in a similar way to the duration of submaximal openings (see main text)

	Cardiac RyR2		Skeletal RyR1	
Variable	Frequency (*n*/s)	Relative F	Frequency (*n*/s)	Relative F
Control	14.3 ± 4.2		14.8 ± 2.4	
1 fM	13.4 ± 4.5	0.73 ± 0.32	18.3 ± 2.7	1.84 ± 0.33*
10 fM	26.5 ± 6.8	2.76 ± 1.05*	19.4 ± 4.2	3.48 ± 1.57
100 fM	36.7 ± 12.5*	4.56 ± 1.43*	28.7 ± 4.3*	4.3 ± 2.04*
1 pM	35.9 ± 11.4*	6.40 ± 2.98*	30.9 ± 2.89*	2.52 ± 0.72*
10 pM	36.8 ± 9.5*	5.56 ± 2.15*	25.4 ± 5.5*	3.36 ± 1.03*
100 pM	20.8 ± 3.3*	5.27 ± 1.74*	29.2 ± 14	5.47 ± 3.64
1 nM	34.2 ± 8.8*	6.16 ± 2.11*	40.7 ± 3.1*	3.13 ± 0.65*
10 nM	28.3 ± 4.4*	5.62 ± 1.58*	nd	nd

Data are presented as average frequency or number of openings per second (*n*/s) and for the average of the frequency in the presence of LITX relative to the frequency before toxin addition, calculated for each individual channel. There is a significant increase in the frequency of openings at concentrations ≥100 fM. nd, RyR1 experiments not performed with 10 nM toxin.

*Significant change from the control parameter value in the presence of the toxin.